Journal of Power Sources 195 (2010) 4785–4795

Contents lists available at ScienceDirect

Journal of Power Sources

journal homepage: www.elsevier.com/locate/jpowsour

An algorithm for sensor-less fuel control of direct methanol fuel cells

Kun-Sheng Shen [a], Chi-Chao Wan [a], Yung-Yun Wang [a], T. Leon Yu [b,c,*], Yu-Jen Chiu [d]

[a] Department of Chemical Engineering, National Tsing Hua University, Hsinchu 30034, Taiwan
[b] Department of Chemical Engineering & Materials Science, Yuan Ze University, Chung-Li, Taoyuan 32003, Taiwan
[c] Fuel Cells Center, Yuan Ze University, Chung-Li, Taoyuan 32003, Taiwan
[d] Department of Mechanical Engineering, Technology and Science Institute of Northern Taiwan, Taipei 11202, Taiwan

ARTICLE INFO

Article history:
Received 12 January 2010
Received in revised form 18 February 2010
Accepted 18 February 2010
Available online 26 February 2010

Keywords:
Fuel control
Sensor-less algorithm
Direct methanol fuel cell

ABSTRACT

We report an algorithm for real-time control of the fuel of a DMFC. The MEA voltage decay coefficients $[e_1, e_2]$, and I–V–T, M'–I–T, and W'–I–T curves (where I is the current, V the voltage, T the temperature, and M' and W' the *methanol* and *water* consumption rates, respectively) of n fuels with specified methanol concentrations $C_{M,k}$ ($k = 1, 2, \ldots, n$) are pre-established and form (I,V,T), (M',I,T), and (W',I,T) surfaces for each $C_{M,k}$. The *in situ* measured $(I,V,T)_u$ after voltage decay correction is applied to the n preset (I,V,T) surfaces to estimate $C_{M,u}$ (the C_M corresponding to $(I,V,T)_u$) using an interpolation procedure. The $C_{M,u}$ is then applied to the n preset (M',I,T) and (W',I,T) surfaces to estimate cumulated "methanol" and "water" consumed quantities . Thus in a real-time system, the C_M and total quantity of fuel can be controlled using the estimated $C_{M,u}$ and cumulated "methanol" and "water" consumed quantities.

© 2010 Elsevier B.V. All rights reserved.

1. Introduction

The direct methanol fuel cells (DMFCs) use dilute methanol aqueous solutions as fuel and are suitable for small or hand-held application systems [1]. In the applications to small and handheld systems, the mass, volume, and efficiency will be the most significant issues to be considered. However, the methanol crossover in a DMFC has been a crucial limitation, which causes a waste of fuel and a reduction of output power when high methanol concentration fuel is fed into the fuel cell units [2]. On the other hand, introducing a low methanol concentration fuel will also lead to a lower output power, because of insufficient fuel. To avoid fuel waste and low output power density, it is desirable to replenish a fuel cartridge with concentrated methanol fuel and pre-dilute inside the DMFC system to an adequate methanol concentration before being fed onto the membrane electrode assemblies (MEAs) to generate current. Thus a fuel (methanol aqueous solution) input control system is needed to regulate the "methanol concentration" and "total quantity" of fuel in a fuel premixing tank before the fuel is fed into the MEA, where the electrochemical reaction takes place.

To regulate the methanol concentration and total quantity of fuel in a premixing tank, one needs the information of the "fuel consumption rate" in a DMFC system. Two system designs were reported in literature [3–6] for estimating fuel consumption rate during operating a DMFC. One is a sensor *in situ* detecting system and the other is a sensor-less regulating system. The sensor *in situ* design consists of a methanol concentration sensor and a liquid level sensor [3]. Using a methanol concentration sensor, one can detect methanol concentration of the fuel in the mixing tank. Using a liquid level sensor, one can measure consumption volume of aqueous fuel in the mixing tank. One can then estimate the methanol and water consumption rates using these two sensors [3,4]. However, liquid level sensor has several disadvantages. First, CO_2 bubble affects detected results of liquid volume in the mixing tank under different operating conditions. Second, there are corrosion and swelling problems on the surface of a liquid level sensor so that periodic replacement of a new sensor and parameter corrections are needed.

In a sensor-less fuel regulating system, one assumes that DMFC works under a stable condition, the only variation during operation is the consumption of fuel, i.e. the decrease of fuel (mixture of methanol and water) in the fuel mixing tank and/or the decrease of methanol concentration of the fuel. No degradation of MEA and damages of current collector and components of the system occur during DMFC is operated. Under these assumptions, the quantity of fuel left in the fuel tank can be estimated from the cell running time and the output potential V and/or current I. And, the concentration of methanol of the fuel can be estimated from the output V and/or I values. The lower V and/or I values than the preceding output ones indicates low methanol concentration of the fuel in the fuel mixing tank. Either the signal of low fuel quantity or low methanol concentration is informed, the fuel regulating system starts to feed fuel

* Corresponding author at: Department of Chemical Engineering & Materials Science, Yuan Ze University, Nei-Li, Taoyuan w32003, Taiwan.
Tel.: +886 3 4638800x2553; fax: +886 3 4559373.
E-mail address: cetlyu@saturn.yzu.edu.tw (T.L. Yu).

0378-7753/$ – see front matter © 2010 Elsevier B.V. All rights reserved.
doi:10.1016/j.jpowsour.2010.02.051

Nomenclature

$[a_{1k}, a_{2k},\ldots, a_{10k}]$ coefficients of a cubic polynomial function $I_k(T,V)$ of $CCS(I,V,T)$ at a constant methanol concentration C_{Mk} ($k = 1, 2, 3,\ldots, n$)
$[b_{1k}, b_{2k},\ldots, b_{10k}]$ coefficients of a cubic polynomial function $M'_k(I,T)$ of $CCS(M',I,T)$ at a constant methanol concentration C_{Mk} ($k = 1, 2, 3,\ldots, n$)
$[c_{1k}, c_{2k},\ldots, c_{10k}]$ coefficients of a cubic polynomial function $W'_k(I,T)$ of $CCS(W',I,T)$ at a constant methanol concentration C_{Mk} ($k = 1, 2, 3,\ldots, n$)
C_M methanol concentration of a fuel
$C_{M,u}$ *in situ* measured C_M
$C_{M,ALP}$ C_M of the liquid fuel after loading a power on the system.
$C_{M,BLP}$ C_M of the liquid fuel before loading a power on the system
$CCS(I,V,T)$ constant concentration surface of (I,V,T), i.e. the surface depicted by I–V curves at various Ts with a constant C_M of fuel
$CCS(M',I,T)$ constant concentration surface of (M',I,T), i.e. the surface depicted by M'–I curves at various Ts with a constant C_M of fuel
$CCS(W',I,T)$ constant concentration surface of (I,V,T), i.e. the surface depicted by W'-I curves at various Ts with a constant C_M of fuel
e_1 MEA temporary voltage decay coefficient
e_2 MEA permanent voltage decay coefficient
I current
I_u *in situ* measured I
$ICCS(I,V,T)$ interpolation algorithm based on $CCS(I,V,T)$
$ICCSs(M',I,T)$ interpolation algorithm based on $CCS(M',I,T)$
$ICCSs(W',I,T)$ interpolation algorithm based on $CCS(W',I,T)$
T temperature
T_u *in situ* measured T
M net methanol consumption flux in anode
M' methanol consumption rate of a fuel
M_{or} methanol consumption flux via oxidation reaction
M_{xover} methanol crossover flux from anode to cathode
M'_u M' corresponding to an *in situ* measured $(I,V,T)_u$ obtained using $ICCSs(M',I,T)$ algorithm
t time interval from the beginning of fuel cell operation to the time of data acquisition
t' time interval starting from the end of an air-starving process to the time of data acquisition
t_{LP} time interval of loading a power on the system
V voltage
V_u *in situ* measured V
V_{u0} V_u without including voltage decrement caused from MEA decay
$V_u'(t')$ temporary voltage decay
$V_u''(t)$ permanent voltage decay
$V_u(t,t')$ V_u including V_{u0}, $V_u'(t')$, and $V_u''(t)$
V_{ALP} total volume of the liquid fuel after loading a power on the system
V_{BLP} total volume of the liquid fuel before loading a power on the system
W net water consumption flux in anode
W' *water* consumption rate of a fuel
W_{or} water consumed flux via oxidation reaction
W_{xover} water crossover flux from anode to cathode
W'_u W' corresponding to an *in situ* measured $(I,V,T)_u$ obtained using $ICCSs(W',I,T)$ algorithm

into the fuel premixing tank and regulate methanol concentration of the fuel to optimize fuel cell output performance [5–6]. Thus, how to control methanol concentration of input fuel and the quantity of fuel in the fuel premixing tank of a DMFC with a sensor-less fuel regulating system for small and portable appliances is one of the key techniques for the commercialization of DMFC.

By assuming no degradation of MEA and no damage of current collector and components of the system occur during a DMFC is operated, Chiu and Lien [7] developed a sensor-less interpolation algorithm based on constant concentration surfaces (*ICCS* algorithm) to estimate methanol concentration of fuel in the premixing tank of a DMFC system. For a given DMFC under a stable operating condition (i.e. no degradations of MEA and cell components), the I–V polarization curve depends only on the cell temperature T and fuel methanol concentration C_M. Thus the I–V polarization curve can be written as [7]:

$$f(I, V, T, C_M) = 0 \tag{1}$$

Eq. (1) indicates that three of the four variables are independent and the rest should be compliant with the equation. In Eq. (1), if C_M is specified as a fixed C_{M0}, then a series of I–V curves can be acquired corresponding to various Ts. By depicting the I–V curves with same C_{M0} in a three-dimensional measurement space with its axis being I, V, and T, a surface spanned by I–V curves corresponding to a fixed C_{M0} can be obtained (see Fig. 1 of Ref. [7]). The surface is defined as a Constant Concentration Surface $CCS(I,V,T)$ with a fuel concentration C_{M0}. Once the $CCSs(I,V,T)$ with various known C_{M0}s are established, the unknown fuel methanol concentration C_u corresponding to an *in situ* measured (I_u,V_u,T_u) datum point can be obtained by interpolation from the pre-established $CCSs(I,V,T)$ (see Fig. 2 of Ref. [7]). The interpolation algorithm based on $CCSs(I,V,T)$ is defined as an $ICCS(I,V,T)$ algorithm.

However to keep a DMFC working in a long period and under an optimum condition, one needs not only to control methanol concentration but needs also to control quantity of the liquid fuel in the fuel premixing tank. Thus an algorithm for *in situ* estimating cumulated fuel consumption quantity is necessary for a sensor-less fuel regulating system. Unfortunately, Chiu and Lien did not report the algorithm for *in situ* estimating fuel consumption quantity in their previous paper. Another problem for applying Chiu and Lien $ICCS(I,V,T)$ algorithm for *in situ* estimating methanol concentration of fuel in a fuel premixing tank of a DMFC under a long period operation is that *ICCS* algorithm was developed based on the assumption that no MEA degradation occurs during long period operation. In a real system, the MEA decay occurs after a long period operation. Thus error of methanol concentration estimation occurs due to MEA decay.

The purpose of this paper is to develop a sensor-less algorithm for real-time controlling methanol concentration and total quantity of fuel in the fuel premixing tank of a DMFC system. The development of the algorithm is based on Chiu and Lien $ICCS(I,V,T)$ algorithm, including: (1) Modification of Chiu and Lien $ICCS(I,V,T)$ algorithm by counting the "MEA decay" into the fuel concentration estimation; (2) Developing $ICCS(M',V,T)$ and $ICCS(W',V,T)$ algorithms (where M' and W' are methanol and water consumption rates, respectively) for *in situ* estimating methanol and water consumption rates; (3) *In situ* estimating "total methanol and total water consumption quantities" by cumulating the data of operating time, methanol consumption rate, and water consumption rate; (4) Developing "methanol" and "water" feed control program to maintain optimum fuel quantity and optimum methanol concentration based on the *in situ* estimated cumulated fuel consumption quantity and methanol concentration in the fuel mixing tank.

2. Brief review of Chiu and Lien *ICCS*(*I*,*V*,*T*) algorithm

Since the present fuel control algorithm is developed based on Chiu and Lien *ICCS*(*I*,*V*,*T*), in this section we briefly review Chiu and Lien *ICCS*(*I*,*V*,*T*) algorithm.

A number of *CCSs* corresponding to the specified methanol concentrations C_{Mk} (where the subscript M indicates methanol and subscript $k = 1, 2, 3, \ldots, n$) of liquid fuels are pre-established experimentally under various temperatures. The *CCSs* are defined as follows:

$$f(I, V, T, C_M)|_{C_M = C_{Mk}} = g_k(I, V, T) = 0 \tag{2}$$

where $k = 1, 2, 3, \ldots, n$.

The function g_k for a liquid fuel with a fixed methanol concentration C_{Mk} can be approximated using a cubic polynomial as shown in Eq. (3):

$$\begin{aligned} g_k(I, V, T) = I - (&a_{1k} + a_{2k}T + a_{3k}V + a_{4k}T^2 + a_{5k}TV + a_{6k}V^2 \\ &+ a_{7k}T^3 + a_{8k}T^2V \\ &a_{9k}TV^2 + a_{10k}V^3) = 0 \end{aligned} \tag{3}$$

where $a_{1k}, a_{2k}, \ldots, a_{10k}$ are coefficients to be determined. Under a constant C_{Mk}, one can measure (I_i, V_i, T_i) for $i = 1, 2, \ldots, m$ at various T and V (or I) and substitute all the values into Eq. (3) to have a set of polynomial equations consisting of coefficients $a_{1k}, a_{2k}, \ldots, a_{10k}$. Then the Least-Squares method can be adopted to solve $[a_{1k}, a_{2k}, \ldots, a_{10k}]$. Therefore, only 10 coefficients $[a_{1k}, a_{2k}, \ldots, a_{10k}]$ are needed to be stored for each $C_{M,k}$ in the fuel cell management system instead of the whole experimental data base. All the data acquisition and relevant computations can be performed beforehand to create a number of *CCSs*(*I*,*V*,*T*) corresponding to each given $C_{M,k}$. The values of $[a_{1k}, a_{2k}, \ldots, a_{10k}]$ corresponding to each $C_{M,k}$ of a fuel in the premixing tank are then stored in the fuel control system of a fuel cell to represent pre-established *CCSs*(*I*,*V*,*T*).

The n series pre-established *CCSs*(*I*,*V*,*T*) data base are used for *in situ* estimating methanol concentration $C_{M,u}$ in the fuel premixing tank using the *in situ* measured (I_u, V_u, T_u) data, where I_u, V_u, T_u are the *in situ* measured I, V, and T, respectively, corresponding to $C_{M,u}$. The interpolation (*ICCS*) procedure is used for estimating $C_{M,u}$ from (I_u, V_u, T_u) data. A measured point $P_u(I_u, V_u, T_u)$ in (I,V,T) space should have n projection points $Q_k(I_k, V_u, T_u)$ on the pre-established $CCS(I_k, V_k, T_k)$ (where $k = 1, 2, 3, \ldots, n$) along the I axis. From Eq. (3), the projection point Q_k has a value of current I_k and can be written as:

$$\begin{aligned} I_k(T_u, V_u) = a_{1k} + a_{2k}T_u + a_{3k}V_u + a_{4k}T_u^2 + a_{5k}T_uV_u + a_{6k}V_u^2 + a_{7k}T_u^3 \\ + a_{8k}T_u^2V + a_{9k}T_uV_u^2 + a_{10k}V_u^3 \end{aligned} \tag{4}$$

Then the unknown methanol concentration $C_{M,u}$ of an inlet fuel corresponding to (I_u, V_u, T_u) can be determined using Lagrange interpolation formula [7].

$$C_{m,u} = \sum_{k=1}^{n} \left(\prod_{\substack{i=1 \\ i \neq k}}^{n} \frac{I_u - I_i}{I_k - I_i} \right) \cdot C_{M,k} \tag{5}$$

In Eq. (5), $I_k = I_k(T_u, V_u)$ and $I_i = I_i(T_u, V_u)$. Accordingly, the *ICCS* algorithm has an *in situ* and unique estimation of the methanol concentration of a liquid-feed fuel cell system, merely by measuring the operating I, V, and T. These are all easily acquired throughout the operating region.

3. Performance decay correction of *ICCS*(*I*,*V*,*T*) algorithm

Since the *in situ* estimation of C_M of a liquid fuel using Chiu and Lien *ICCS*(*I*,*V*,*T*) algorithm is based on the assumption that no MEA decay occurs during the operation of DMFC. The output V_u values should be constant if the corresponding I_u, T_u, and $C_{M,u}$ are constants. However, in a real system the output V_u values might be lowered due to MEA decay. The lowered output V_u value causes an under-estimating of C_M of the liquid fuel using *ICCS*(*I*,*V*,*T*) algorithm. Thus, we need to make corrections of the measured V_u data to minimize the errors caused from MEA decay. The corrected V_{u0} data can then be input into Eqs. (4) and (5) of *ICCS*(*I*,*V*,*T*) algorithm to precisely estimate the C_M of a liquid fuel.

The decay of fuel cell performance can be attributed to two categories. One is "permanent performance decay", the other is "temporary performance decay". The permanent decay of a DMFC can be attributed to: (a) the decay of electro-catalysis activities of anode and cathode catalysts; (b) the decay of cathode hydrophobic behaviour; (c) crossover of ruthenium catalyst from anode through polyelectrolyte membrane (PEM) to cathode; and (d) degradations of PEM and interfaces of MEA [8]. The temporary performance decay of a DMFC is caused by: (a) the flooding of GDL, and (b) the decay of cathode catalysis activity due to the formation of platinum oxide on the surfaces of *Pt* particles [9]. In a DMFC, the permanent decay is not reversible and can not be recovered. However, the temporary decay is reversible and can be recovered. Eickes et al. [9] had shown that after 2 h of continuous operation the cathode *Pt* particles surfaces were saturated with platinum oxide. The oxidized platinum can be reduced to its catalytic form by air-starving the cathode to consume the remaining oxygen in the oxidation of crossover methanol. Thus the DMFC needs temporary unloading for 30 s to reduce platinum oxide saturated on the surfaces of cathode *Pt* particles for every 2 h (i.e. 7200 s) of continuous operation. Because of temporary decay and permanent decay of MEA, we need to make correction of the measured output voltage V_u when using *ICCS*(*I*,*V*,*T*) algorithm to estimate C_M of the liquid fuel in the fuel premixing tank.

In the present DMFC long time operation study, we followed Eickes et al. air-starving procedure unloading DMFC for 30 s to recover Pt catalyst activity for every 2 h of operation. As will be shown in Section 7.1.3, Figs. 5 and 6, both temporary voltage decay $V_u'(t')$ and permanent voltage decay $V_u''(t)$ are linear dependent on DMFC operating time and can be approximated as $V_u'(t') = -e_1 t'$ and $V_u''(t) = -e_2 t$. Where t' is the time interval starting from the end of each air-starving process (reduction of *Pt oxide* covered on surfaces of cathode catalyst particles) to the time of data acquisition, t the time interval from beginning of fuel cell operation to the time of data acquisition, e_1 the empirical coefficient relating to voltage decrement caused from temporary MEA decay, and e_2 the empirical coefficient relating to voltage decrement caused from permanent MEA decay. The voltage $V_u(t,t')$ including $V_u'(t')$ and $V_u''(t)$ can be expressed as:

$$\begin{aligned} V_u(t, t') &= V_{u0} + V_u'(t') + V_u''(t) \\ &= V_{u0} - e_1 t' - e_2 t \end{aligned} \tag{6}$$

with $t' = 0 \rightarrow 7200$ s and $t = 0 \rightarrow \infty$ s

In Eq. (6), V_{u0} is the V_u without including any voltage decrement caused from MEA decay. The reason for the time set of $t' = 0 \rightarrow 7200$ s is because the cathode *Pt* needs 30 s air-starving process to recover cathode catalyst activity for every 2 h (i.e. 7200 s) of DMFC operation and the time t' needs to restart from 0 s after each air-starving process [9]. The coefficients e_2 and e_1 can be obtained from linear curve fitting of a preset experimental data (as will be shown in Figs. 5 and 6) and stored in the fuel control system of a DMFC. The *in situ* measured $V_u(t,t')$ data can then be input into Eq. (6) to obtain the corrected voltage V_{u0} value. The corrected V_{u0} value instead of

V_u can then be input into in the *ICCS* algorithm Eqs. (4) and (5) to estimate $C_{M,u}$ of the liquid fuel in the premixing tank.

4. The algorithm for estimating fuel consumption rate

4.1. Establishment of CCS(M′,I,T) and CCS(W′,I,T)

In general, the fuel at anode of a DMFC is consumed via two routes. One is the electrochemical oxidation reaction and other is the fuel crossover through PEM. The net flows of methanol and water are described in Eqs. (7) and (8), respectively [10].

$$M = M_{or} + M_{xover} \tag{7}$$

$$W = W_{or} + W_{xover} \tag{8}$$

where M is the net consumption flux of methanol in anode, M_{or} the methanol consumed via oxidation reaction Eq. (9), M_{xover} the methanol crossover from anode to cathode, W the net consumption flux of water in anode, W_{or} the water consumed via oxidation reaction Eq. (9), and W_{xover} the water crossover from anode to cathode. Eq. (9) shows the methanol and water oxidation reaction at anode.

$$CH_3OH + H_2O \rightarrow 6H^+ + 6e^- + CO_2 \tag{9}$$

The fuel consumption rate via oxidation reaction (i.e. Eq. (9)) at anode depends on the operating current I. The water and methanol crossover through PEM occurs via three processes, i.e. diffusion, hydraulic permeation, and electro-osmotic drag [11–13]. It is known that diffusions, hydraulic permeations, and electro-osmotic drags of water and methanol are all T dependent. Besides depending on T, the diffusion coefficients of water and methanol also depend on C_M of liquid fuel. The water consumption rate W' via diffusion process decreases and the methanol consumption rate M' via diffusion process increases with increasing C_M of liquid fuel. The electro-osmotic drag coefficients of water and methanol are also I dependent [10,14].

Hence for a portable DMFC system working in an ambient environment, M' and W' depend only on C_M, T, and I [10,11,14], and are functions of C_M, T, and I as shown in Eqs. (10) and (11).

$$\frac{dM}{dt} = M' = h_M(C_M, T, I) \tag{10}$$

$$\frac{dW}{dt} = W' = h_W(C_M, T, I) \tag{11}$$

By keeping the C_M of the fuel in a premixing tank at a constant value, i.e. $C_{M,k}$, the W' and M' can be measured experimentally at various T and I. Then a preset of M'–I–T and W'–I–T curves can be obtained experimentally to generate $CCS(M',I,T)_k$ and $CCS(W',I,T)_k$ with $C_M = C_{M,k}$. Thus, presets of $CCS(M',I,T)_k$ *and* $CCS(W',I,T)_k$ can then be generated for various $C_{M,k}$ with $k = 1, 2, 3, \ldots, n$. The *CCSs* are defined as following:

$$f(M', I, T, C_M)|_{C_M = C_{M,k}} = h_{k,M}(M', I, T) = 0 \tag{12}$$

$$f(W', I, T, C_M)|_{C_M = C_{M,k}} = h_{k,W}(W', I, T) = 0 \tag{13}$$

Both M' and W' are functions of T and I at $C_M = C_{M,k}$. Similar to Eq. (3), we can develop two cubic polynomials for $M'_k(T, I)$ and $W'_k(T, I)$ for each $C_{M,k}$. The cubic polynomials of $M'_k(T, I)$ and $W'_k(T, I)$ consist of coefficients $[b_{1k}, b_{2k}, \ldots, b_{10k}]$ and $[c_{1k}, c_{2k}, \ldots, c_{10k}]$, respectively, to be determined. Under a constant C_{Mk}, one can measure (M_i', I_i, T_i) and (W_i', I_i, T_i) for $i = 1, 2, \ldots, m$ at various I and T and substitute all the values into cubic polynomials of $M'_k(T, I)$ and $W'_k(T, I)$. Then the Least-Squares method can be adopted to solve $[b_{1k}, b_{2k}, \ldots b_{10k}]$ and $[c_{1k}, c_{2k}, \ldots, c_{10k}]$. Therefore, only 20 coefficients $[b_{1k}, b_{2k}, \ldots, b_{10k}]$ and $[c_{1k}, c_{2k}, \ldots, c_{10k}]$ are needed to be stored for each $C_{M,k}$ in the fuel cell management system. All the data acquisition and relevant computations can be performed beforehand to create a number of $CCS(M',I,T)$ *and* $CCS(W',I,T)$ corresponding to each given $C_{M,k}$. The values of $[b_{1k}, b_{2k}, \ldots, b_{10k}]$ and $[c_{1k}, c_{2k}, \ldots c_{10k}]$ corresponding to each $C_{M,k}$ (with $k = 1, 2, 3, \ldots, n$) of a fuel in the premixing tank are then stored in the fuel control system of a DMFC to represent pre-established $CCS(M',I,T)$ and $CCS(W',I,T)$, respectively.

4.2. Procedures of interpolating CCS(M′,I,T) and CCS(W′,I,T) (ICCS(M′,I,T) and ICCS(W′,I,T)) to estimate methanol and water consumption rates

After the n series of coefficients $[a_{1k}, a_{2k}, \ldots, a_{10k}]$ of $CCSs(I_k,V_k,T_k)$, coefficients $[b_{1k}, b_{2k}, \ldots, b_{10k}]$ of $CCSs(M_k',I_k,T_k)$, and coefficients $[c_{1k}, c_{2k}, \ldots, c_{10k}]$ of $CCSs(W_k',I_k,T_k)$ corresponding to $C_{M,k}$ (with $k = 1, 2, 3, \ldots, n$) and the voltage decay coefficients $[e_1, e_2]$ are established and stored in the fuel control system of a DMFC, one can carry out *in situ* estimation of M_u' and W_u' from the measured (I_u,V_u,T_u) data. The similar interpolation procedures described in Section 2 are used for M_u' and W_u' estimation.

A measured point with its V_u corrected using Eq. (6), i.e. $P_u(I_u, V_{u0}, T_u)$, in (I,V,T) space should have n set of projection points $Q_{I,k}$, $Q_{M',k}$, and $Q_{W',k}$ on each of the pre-established $CCS(I_k,V_k,T_k)$, $CCS(M_k',I_k,T_k)$, and $CCS(W_k',I_k,T_k)$, respectively, each with a C_M relating to $C_{M,k}$ ($k = 1, 2, \ldots, n$). Each of the projection points $Q_{I,k}$, $Q_{M',k}$, and $Q_{W',k}$ has a value of $I_k(V_{u0},T_u)$, $M_k'(I_u,T_u)$ and $W_k'(I_u,T_u)$, respectively. As shown in Section 2, the $I_k(V_{u0},T_u)$ value can be calculated using Eq. (4) with the pre-stored coefficients $[a_{1k}, a_{2k}, \ldots, a_{10k}]$. Similar to the procedures of calculating $I_k(V_{u0},T_u)$, $M_k'(I_u,T_u)$ and $W_k'(I_u,T_u)$ can also be calculated using the similar cubic polynomials as shown in Eq. (4) with the pre-stored coefficients $[b_{1k}, b_{2k}, \ldots, b_{10k}]$ and $[c_{1k}, c_{2k}, \ldots, c_{10k}]$, respectively. In using Eq. (4) to calculate $M_k'(I_u,T_u)$ and $W_k'(I_u,T_u)$, variables V_u and T_u of Eq. (4) are replaced with I_u and T_u, and the coefficients $[a_{1k}, a_{2k}, \ldots, a_{10k}]$ of Eq. (4) are replaced with $[b_{1k}, b_{2k}, \ldots, b_{10k}]$ and $[c_{1k}, c_{2k}, \ldots, c_{10k}]$, respectively. Before proceeding interpolation procedures to estimate M_u' and W_u', we need to estimate $C_{M,u}$. By input I_u, $I_k(V_{u0},T_u)$, and $C_{M,k}$ ($k = 1,2, \ldots, n$) data into Eq. (5), one can compute $C_{M,u}$. Then M_u' and W_u' can be determined by input $C_{M,u}$, and $M'_k(I_u,T_u)$, and $W'_k(I_u,T_u)$ ($k = 1,2, \ldots, n$) into interpolation Eqs. (14) and (15), respectively.

$$M_u' = \sum_{k=1}^{n} \left(\prod_{\substack{i=1 \\ i \neq k}}^{n} \frac{C_{M,u} - C_{M,i}}{C_{M,k} - C_{M,i}} \right) \cdot M_k' \tag{14}$$

$$W_u' = \sum_{k=1}^{n} \left(\prod_{\substack{i=1 \\ i \neq k}}^{n} \frac{C_{M,u} - C_{M,i}}{C_{M,k} - C_{M,i}} \right) \cdot W_k' \tag{15}$$

In Eqs. (14) and (15), $C_{M,k}$ and $C_{M,i}$ are the C_Ms of the projections of the corrected point (I_u,V_{u0},T_u) on the pre-established $CCS(I_k,V_k,T_k)$ of $C_{M,k}$ and $CCS(I_i,V_i,T_i)$ of $C_{M,i}$, respectively. And, M_k' and W_k' are $M'_k(I_u,T_u)$, and $W'_k(I_u,T_u)$, respectively, corresponding to $C_M = C_{M,k}$.

5. *In situ* estimation of the methanol concentration and the cumulated methanol and water consumed quantities of liquid fuel in the premixing tank of DMFC

Once the voltage decay coefficients e_1 and e_2, and coefficients $[a_{1k}, a_{2k}, \ldots, a_{10k}]$ of $CCSs(I,V,T)$, coefficients $[b_{1k}, b_{2k}, \ldots, c_{10k}]$ of $CCS(M',I,T)$, and coefficients $[c_{1k}, c_{2k}, \ldots, c_{10k}]$ of $CCS(W',I,T)$ are established and stored in a DMFC system, one can use these preset data to carry out *in situ* estimations of the cumulated fuel (methanol and water) consumed quantities at any operating time period t. The estimation procedures consist of three steps. The first step is

C_M estimation using *ICCS*(*I*,*V*,*T*) algorithm, the second is M' and W' estimations using *ICCS*(M',*I*,*T*) and *ICCS*(W',*I*,*T*) algorithms, and the third is the calculation of the total cumulated methanol and water consumed quantities during an operating time period *t*.

The procedures for *in situ* estimating methanol concentration of fuel in the premixing tank and cumulated fuel consumed quantities of an operating DMFC for fuel control are: (1) carry out (I_u,V_u,T_u) measurements during operating a DMFC; (2) make MEA performance corrections of V_u using Eq. (6) and preset e_1 and e_2 coefficients to obtain corrected V_{u0}; (3) input I_u, T_u and corrected V_{u0} data into modified *ICCS*(*I*,*V*,*T*) algorithm to obtain $C_{M,u}$; (4) input I_u, T_u and $C_{M,u}$ data into *ICCS*(M',*I*,*T*) and *ICCS*(W',*I*,*T*) algorithms to obtain $M_u{}'$ and $W_u{}'$; (5) calculate the consumed quantities of methanol $M = M_u{}' \times \Delta t$ and water $W = W_u{}' \times \Delta t$ in the time interval Δt (where Δt = the time interval between two estimations); (6) let the total methanol and total water consumed quantities be M_t and W_t, respectively, and sum the methanol and water consumed quantities using the equations: $M_t = M_t + M$ and $W_t = W_t + W$; (7) repeat procedures (1)–(6) and evaluate M_t and W_t till M_t and W_t larger than the fuel levels requiring to refill methanol and water, respectively; (8) fill methanol and water according to the evaluated results of procedure (7).

6. Experimental

6.1. DMFC testing system

A real-time DMFC testing system consisting of a DMFC stack, a water reservoir, a methanol reservoir, a tank for mixing water and methanol, an electronic loading, and a visual BASIC control software designed by Antig Co, Taiwan, was used in the present work. The architecture of the DMFC testing system is shown in Fig. 1. The water and methanol were stored in two separated reservoirs and were pumped into a 30 mL fuel mixing tank before the fuel was fed into anode of the fuel cell stack. A liquid level sensor (Syspotek Inc., Taiwan) was used to detect the fuel volume in the mixing tank and a methanol concentration detector (DA-130N, Japan) was used to measure the methanol concentration before the fuel was injected into the anode of the fuel cell stack. An electronic load (Chroma 63030, Chroma Co, Inc., Taiwan) was used as a constant power load and an ultra-mobile personal computer was used as a dynamic power load. The DMFC stack (Apolo® stack, Antig Inc., Taiwan) consisted of 32 unit cells. The membrane electrode assembly (MEA) in each unit cell was a Nafion-117 based MEA with an active area of 3.5x3.5 cm^2. The anode catalyst was Pt-Ru/C and the cathode catalyst was Pt/C. The Pt loadings at anode and cathode of each MEA were 2 mg cm^{-2} and 2 mg cm^{-2}, respectively.

6.2. Data acquisitions for establishing CCSs(I,V,T)

The DMFC *I*–*V* measurements were carried out using standard testing procedures under a constant voltage mode. Preheating methanol aqueous solution was fed into anode with a flow rate of 120 mL min^{-1}, and the air without compression was fed into cathode with a flow rate of 10 L min^{-1}. *I*–*V* curves were obtained by measuring the current *I* with step decrement of voltage from 11.2 V to 8.0 V by an interval of 0.32 V (0.01 V per unit cell). The time interval for each measurement was held for 1 min. The *I*–*V* data of five inlet liquid fuels with C_Ms = 2.0 vol.%, 3.0 vol.%, 4.0 vol.%, 5.0 vol.%, and 6.0 vol.% were obtained at 30, 40, 50, and 60 °C, and these data were used to establish five *CCSs*(*I*,*V*,*T*) with C_M = 2.0 vol.%, 3.0 vol.%, 4.0 vol.%, 5.0 vol.%, and 6.0 vol.%.

6.3. Estimations of temporary and permanent voltage decay coefficients e_1 and e_2

The voltage *V* of the DMFC stack was measured with a duration time of 15 min at two operating conditions: (a) Temp = 60 °C, *I* = 2.5 A, and C_M = 6.0 vol.%; and (b) Temp = 40 °C, *I* = 1.0 A, and C_M = 4.0 vol.%. The flow rate of liquid fuel into anode was 120 mL min^{-1} and the air flow rate into cathode was 10 L min^{-1}. The DMFC system was operated for 1000 h (i.e. 1000 h is the duration time of *t* of Eq. (6)). During operation, the system was temporary unloading for 30 s for every 2 h to recover catalysis activity of cathode *Pt* catalyst by air-starving process as described in Section 3 (where *2* h is the duration time of t' of Eq. (6)). The experimental data were then input into Eq. (6) to calculate temporary and permanent voltage decay coefficients e_1 and e_2.

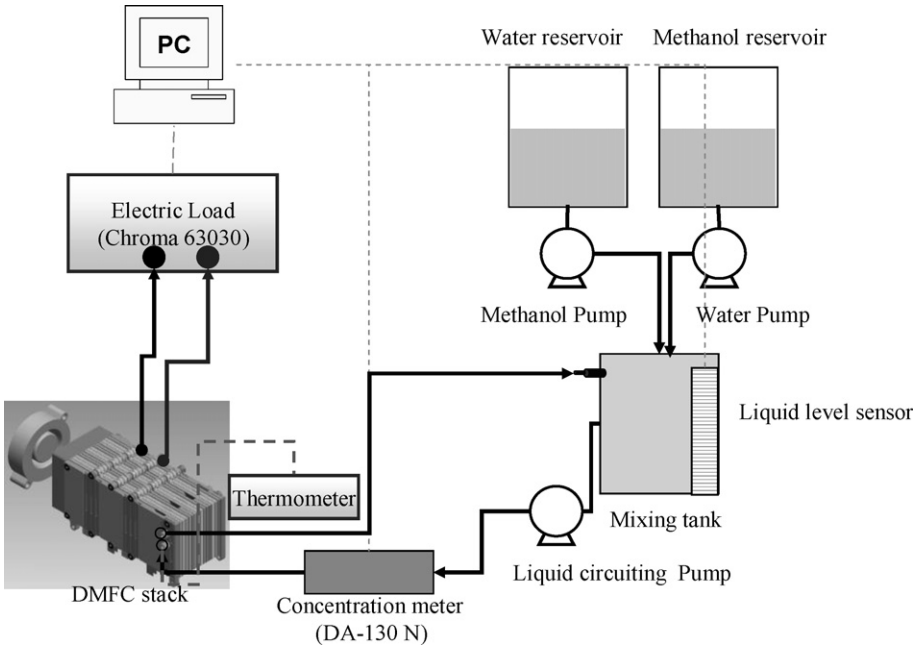

Fig. 1. The architecture of a DMFC testing system.

6.4. Data acquisitions for establishing CCSs(M′,I,T) and CCSs(W′,I,T)

The W' and M' data were measured at five currents I = 0.5, 1.0, 1.5, 2.0, and 2.5 A, four temperatures T = 30 °C, 40 °C, 50 °C, and 60 °C, and four liquid fuels with C_M = 4.0 vol.%, 5.0 vol.%, 6.0 vol.%, and 8.0 vol.%. The power loading time of each measurement was 30 min and the liquid fuel flow rate was 120 mL min^{-1}. In order to keep a constant C_M during the whole period of measurement, the fuel exhausted from the outlet of cathode was not circulated back to the fuel reservoir. The densities of fuels in the fuel mixing tank were measured using a density meter (Anton Paar 4100). The C_Ms of fuels were then estimated from their *densities* using a C_M versus *density* calibration curve obtained from methanol aqueous solutions with known C_Ms. The fuel consumption rates M' and W' were the methanol and water consumed quantities, respectively, in an unit power loading time, and can be calculated using the following equations:

$$\frac{dM}{dt} = M' = \frac{V_{BLP} \times C_{M,BLP} - V_{ALP} \times C_{M,ALP}}{t_{LP}} \quad (16)$$

$$\frac{dW}{dt} = W' = \frac{V_{BLP} \times (1 - C_{M,BLP}) - V_{ALP} \times (1 - C_{M,ALP})}{t_{LP}} \quad (17)$$

where V_{BLP} is the total volume of the liquid fuel before loading a power on the system, V_{ALP} the total volume of the liquid fuel after loading a power on the system, $C_{M,BLP}$ the C_M of the liquid fuel before loading a power on the system, $C_{M,ALP}$ the C_M of the liquid fuel after loading a power on the system, and t_{LP} the time interval of loading a power on the system.

7. Results and discussion

7.1. ICCS(I,V,T) algorithm

7.1.1. Establishment of CCSs(I,V,T)

To avoid ambiguities of the predicting results, the preset *CCSs*(*I*,*V*,*T*) for liquid fuels with various $C_{M,k}$ (where k = 1, 2, 3,. . ., n) should not intersect with each other. Thus feasible measurement regions of C_M of the liquid fuel, operating temperature T, and voltage V for preset *CCSs*(*I*,*V*,*T*) without intersections should be obtained first. The establishment of *CCSs*(*I*,*V*,*T*) with feasible measurement regions for predicting C_M of the inlet fuel of a DMFC unit cell had been reported by Chiu and Lien [7]. They found the feasible measuring regions for predicting C_M of a liquid fuel are: C_M = 3.0–6.0 vol.%, V = 0.10–0.35 V, and T = 30–60 °C. The error of the predicted C_M of a liquid fuel was less than 5.0%. In the present work, we carried out measurements on a DMFC stack consisting of 32 unit cells. The working regions are: C_M = 2.0–6.0 vol.%, V = 8.0–11.2 V (0.25–0.35 V per unit cell), and T = 30–60 °C. The *I*–*V* curves of C_M = 2.0, 3.0, 4.0, 5.0, and 6.0 vol.% and T = 30 °C, 40 °C, 50 °C, and 60 °C are shown in Fig. 2. By inserting the experimental data into Eq. (3) and using Least-Squared method, we obtained the coefficients a_{1k}, a_{2k},. . ., a_{10k} for five $C_{M,k}$ (i.e. $C_{M,k}$ = 2.0, 3.0, 4.0, 5.0, and 6.0 vol.% for k = 1, 2, 3, 4, and 5, respectively). Using the five set [a_{1k}, a_{2k},. . ., a_{10k}] coefficients (k = 1, 2, 3, 4, and 5,), we constructed five fitted *CCSs*(*I*,*V*,*T*). The fitted *CCSs*(*I*,*V*,*T*) are depicted in Fig. 3. No intersection was found among these five *CCSs*(*I*,*V*,*T*), suggesting the working regions of the present *CCSs*(*I*,*V*,*T*) are feasible. These results revealed that the feasible working regions for a stack consisting of 32 unit cells are similar to those of a unit cell.

7.1.2. Evaluation of ICC(I,V,T) algorithm

To evaluate *ICCS*(*I*,*V*,*T*) algorithm, three additional inlet fuels with C_M = 3.5 vol.%, 4.5 vol.%, and 5.5 vol.% were introduced to serve as fuels with unknown methanol concentration $C_{M,u}$. Each of the three C_Ms was assigned 14 measurement points distributed in the temperatures ranging from 30 °C to 60 °C with an increment of 5 °C and two voltages 9.6 V and 8.0 V. Thus 42 set (I_u,V_u,T_u) data were obtained in the three-dimensional (*I*,*V*,*T*) space. Since there are five pre-established *CCSs*(*I*,*V*,*T*) (Fig. 3) with five sets of coefficients [a_{1k}, a_{2k}, . . ., a_{10k}] (k = 1, 2, 3, 4, and 5), we were able to estimate $C_{M,u}$ of each I_u datum by using Eqs. (4) and (5). The comparison between real C_Ms (i.e. C_M = 3.5 vol.%, 4.5 vol.%, and 5.5 vol.%) and the $C_{M,u}$s estimated from pre-established *CCSs*(*I*,*V*,*T*) (Fig. 3) using *ICCS*(*I*,*V*,*T*) algorithm is shown in Fig. 4. Fig. 4 shows the relative errors were less than 5%, indicating the accuracy of present *ICCS*(*I*,*V*,*T*) algorithm for estimating C_M of an inlet fuel of a DMFC stack consisting of 32 unit cells.

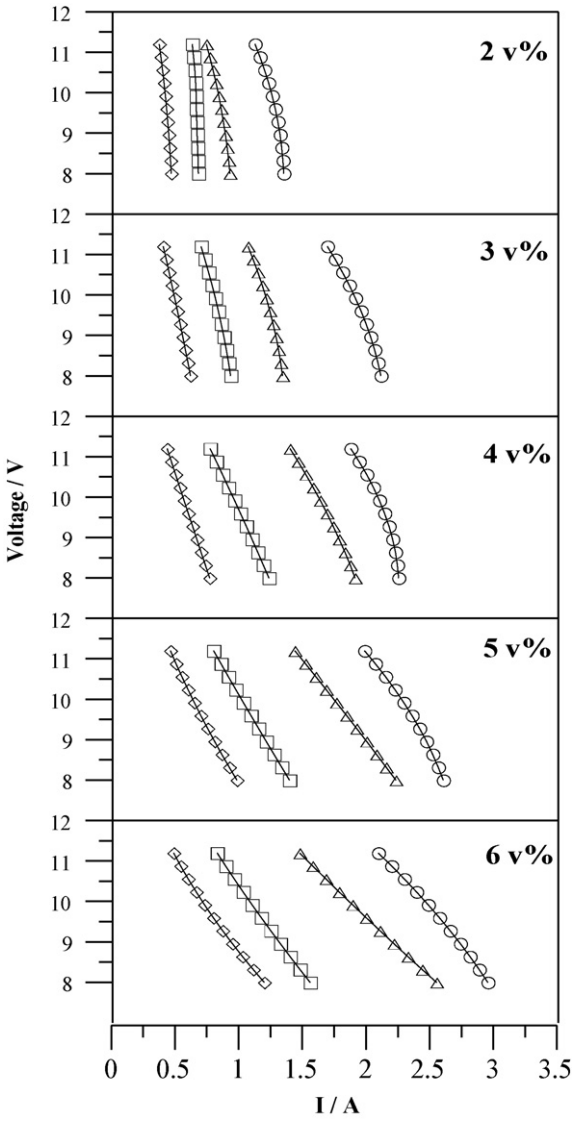

Fig. 2. *I*–*V* curves of a DMFC operated at various temperatures with liquid fuels of various C_M. C_M: 2 vol.%, 3 vol.%, 4 vol.%, 5 vol.%, and 6 vol.% (from top to bottom). Operating temperature: (◊) 30 °C; (□) 40 °C; (△) 50 °C; (○) 60 °C.

7.1.3. Estimation of temporary and permanent voltage decay coefficients e_1 and e_2

To estimate the empirical voltage decay coefficients e_1 and e_2 of Eq. (6) for a long time operating DMFC stack, two set of stack voltage data were collected under two different operating conditions using two freshly prepared stacks. Fig. 5 shows the variation of stack voltage versus operating time for 36×10^5 s

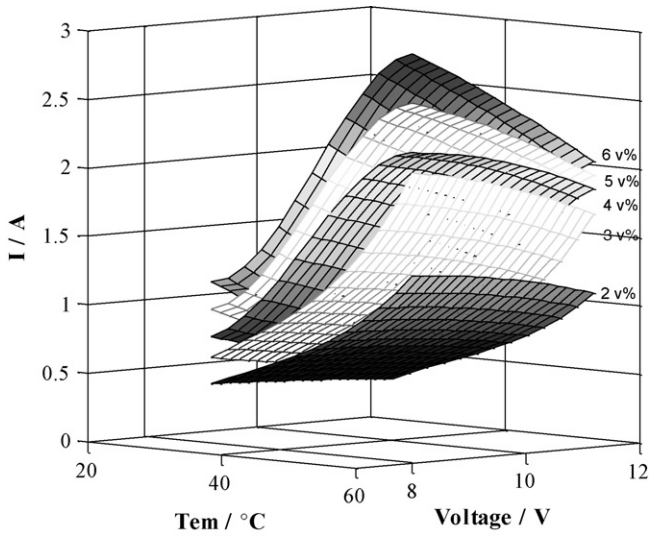

Fig. 3. The fitted *CCSs*(*I*,*V*,*T*) for fuels with C_M = 2.0 vol.%, 3.0 vol.%, 4.0 vol.%, 5.0 vol.%, and 6.0 vol.%. The *CCSs*(*I*,*V*,*T*)were constructed using five set [a_{1k}, a_{2k},. . ., a_{10k}] coefficients (k = 1, 2, 3, 4, and 5), which were obtained by polynomial least-square curve fitting of the data of Fig. 2 using Eq. (3).

(i.e. 1000 h): (a) at 60 °C with I = 2.5 A and an inlet fuel with C_M = 6.0 vol.% and (b) at 40 °C with I = 1.0 A and an inlet fuel with C_M = 4.0 vol.%. These data show voltage fluctuates around +0.36 V for every 7200 s of operation, which was a temporary voltage decay and was recovered by air-starving for 30 s. The bold dashed line along the highest voltage of each fluctuation shown in Fig. 5 indicates permanent voltage decay without temporary decay (i.e. the voltage after recovered by air-starving for 30 sec, $V_u(t,t') = V_{u0} - e_2 t$, with $t' = 0$). The data of Fig. 5a (upper graph) showed a stack voltage decay rate of $e_2 = 0.0285 \times 10^{-5}$ V s^{-1}, and those of Fig. 5b (lower graph) showed a stack voltage decay rate of $e_2 = 0.0290 \times 10^{-5}$ V s^{-1}. These results suggest that within the operating region, T = 40–60 °C, I = 1.0–2.5 A, and C_M = 4.0–6.0 vol.%, the rate of permanent voltage decay was almost a constant with an average $e_2 = (0.0288 + 0.0003) \times 10^{-5}$ V s^{-1}.

Rearranging Eq. (6), we obtain:

$$V_u(t, t') + e_2 t = V_{u0} - e_1 t' \quad (18)$$

Using the experimental $V_u(t, t')$ data and e_2 data obtained from Fig. 5a and b, we are able to plot $[V_u(t, t') + e_2 t]$ versus t' of Eq. (18) and the temporary voltage decay coefficient e_1 can be obtained from the slope of the plot. We took voltage data of three fuel

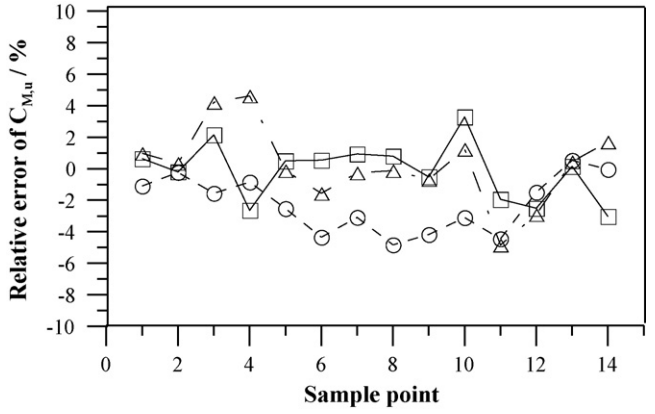

Fig. 4. Relative errors of $C_{M,u}$ data which were calculated from 42 set of (I_u,V_u,T_u) testing data using *ICCS*(*I*,*V*,*T*) algorithm (Eqs. (4) and (5)) and preset *CCSs*(*I*,*V*,*T*) of Fig. 3. The real C_M of inlet fuels: (○) 3.5 vol.%; (△) 4.5 vol.%; (□) 5.5 vol.%.

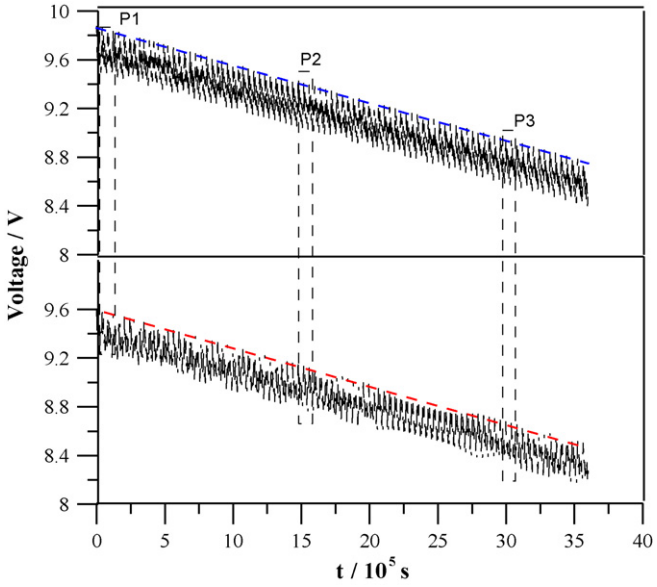

Fig. 5. Plots of $V_u(t,t')$ versus t (Eq. (6)) of a fuel cell stack operated for 36×10^5 s (i.e. 1000 h). The bold dashed line indicates permanent voltage decay without temporary voltage decay (i.e. the voltage after recovering *Pt* catalysis by air-starving for 30 s, $V_u(t,t') = V_{u0} - e_2 t$, with $t' = 0$). (a, upper graph) I = 2.5 A, C_M = 6.0 vol.%, T = 60 °C, $e_2 = 0.0285 \times 10^{-5}$ V s^{-1}; (b, lower graph) I = 1.0 A, C_M = 4.0 vol.%, T = 40 °C, $e_2 = 0.0290 \times 10^{-5}$ V s^{-1}.

cell operating periods *P1*, *P2*, and *P3* as indicated in Fig. 5a and b and the average coefficient $e_2 = 0.0288 \times 10^{-5}$ V s^{-1} estimated in Fig. 5 to calculate $[V_u(t, t') + e_2 t]$ data. Fig. 6 shows the plots of $[V_u(t, t') + e_2 t]$ versus t' of the three fuel cell operating periods *P1*, *P2*, and *P3*. Each plot has a duration time of 7200 s, which is the time interval between two sequential air-starving processes for *Pt* catalysis recovering. These data show the temporary voltage decay curves had almost the same slope in the three fuel cell operating periods, suggesting the fuel cell had similar temporary decay behaviour during the long time operation for 36×10^5 s at the operating region: T = 40–60 °C, I = 1.0–2.5 A, and C_M = 4.0–6.0 vol.%. The e_1 values estimated from the plots of Fig. 6 had an average value of $e_1 = (5.1 + 0.04) \times 10^{-5}$ V s^{-1}. With the coefficients e_1 and e_2, the corrected voltage V_{u0} can be calculated from experimental data $V_u(t, t')$ using Eq. (6). The corrected voltage V_{u0} datum instead of V_u is then input into the *ICCSs*(*I*,*V*,*T*) algorithm Eqs. (4) and (5) to estimate C_M of an inlet liquid fuel.

7.2. *ICCSs(M′,I,T) and ICCSs(W′,I,T) algorithms*

7.2.1. *Establishment of CCSs(M′,I,T) and CCSs(W′,I,T)*

The M' and W' data were measured at I = 0.5, 1.0, 1.5, 2.0, and 2.5 A, and T = 30 °C, 40 °C, 50 °C, and 60 °C with C_M of liquid fuels of 4.0 vol.%, 5.0 vol.%, 6.0 vol.%, and 8.0 vol.%. The M' and W' data were plotted against I at four temperatures with four C_Ms and are shown in Figs. 7 and 8, respectively. Fig. 7 shows M' increases with increasing I, T, and C_M. The increment of I, C_M, and T in a DMFC system results in an increase in electrochemical reaction rate and thus an increase in M'. The increases of C_M and I also results in an increment in methanol crossover via diffusion and via electro-osmosis, respectively, and thus an increase in M'. Fig. 8 shows that W' has similar I and T dependencies as M', i.e. W' increases with increasing I and/or T. However, Fig. 8 shows W' decreases slightly with increasing C_M when the fuel cell was operated at fixed I and T. This behaviour is opposite to the C_M dependency of M'. As shown in Fig. 7, M' increases with increasing C_M at fixed I and T.

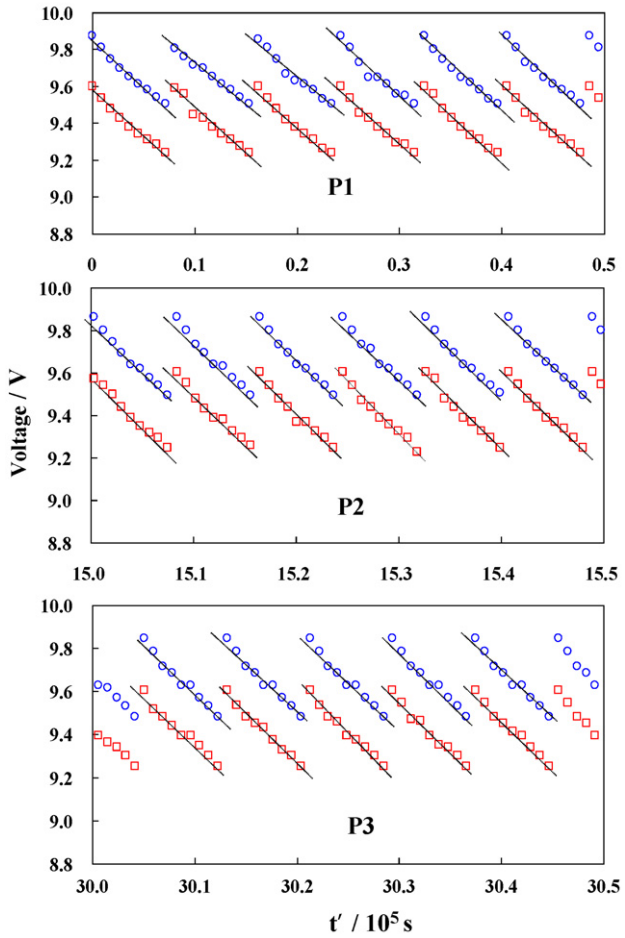

Fig. 6. Plots of $[V_u(t, t') + e_2 t]$ versus t' of the three fuel cell operating periods *P1*, *P2*, and *P3* as indicated in Fig. 6a and b. (◯) Fuel cell stack operated at $T = 60\,^{\circ}C$, $I = 2.5$ A, $C_M = 6.0$ vol.%; (□) Fuel cell stack operated at $T = 40\,^{\circ}C$, $I = 1.0$ A, $C_M = 4.0$ vol.%. The e_1 value estimated from the slopes of these plots has an average $e_1 = (5.10 + 0.04) \times 10^{-5}$ V s^{-1}.

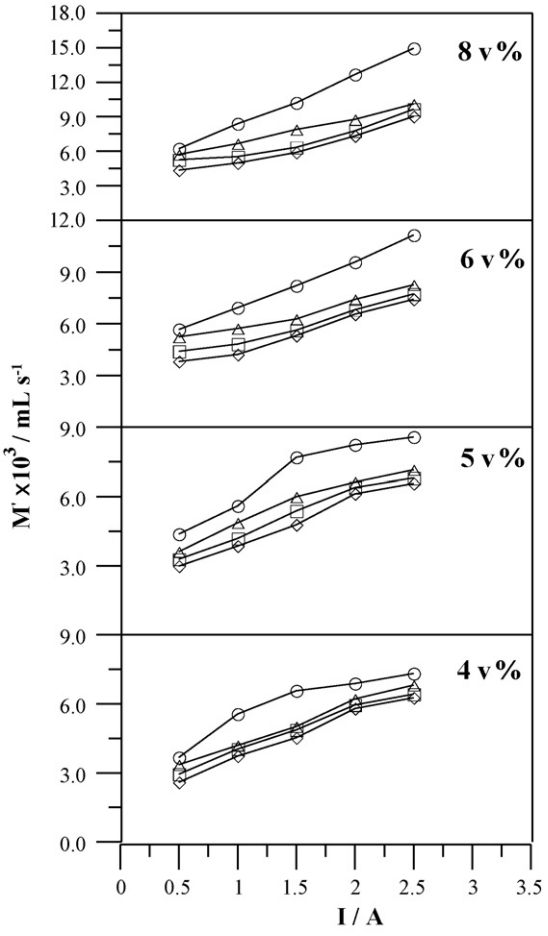

Fig. 7. M' versus I curves obtained at various temperatures with C_M of liquid fuels of 4.0 vol.%, 5.0 vol.%, 6.0 vol.%, and 8.0 vol.% (from bottom to top). Temperature: (◊) 30 °C; (□) 40 °C; (△) 50 °C; (◯) 60 °C.

Comparing the data of Fig. 8 with those of Fig. 7, we also found that at fixed I and T, the variation of W' with increasing C_M is smaller than that of M' with increasing C_M. This phenomenon suggests that the C_M dependency of W' is not so strong as that of M'. Kang et al. [10] developed a mass balance model of DMFC and carried out methanol and water crossover and methanol utilization measurements. Their results were similar to our present work. As the C_M of fuel increased, the water crossover decreased since lower anode water flow rate and higher methanol crossover. The higher methanol crossover caused a higher methanol concentration gradient and a lower water concentration gradient within the electrolyte membrane.

By replacing (I,V,T) of Eq. (3) with (M',I,T), respectively, M' can be approximated as a cubic polynomial of I and T with coefficients $[b_{1k}, b_{2k}, \ldots, b_{10k}]$. Similarly, by replacing (I,V,T) of Eq. (3) with (W',I,T), respectively, W' can also be approximated as a cubic polynomial of I and T with coefficients $[c_{1k}, c_{2k}, \ldots, c_{10k}]$. Inserting the experimental (M',I,T) and (W',I,T) data obtained at $C_M = 4$ vol.%, 5 vol.%, 6 vol.%, and 8 vol.% into the cubic polynomials of $M'(I,T)$ and $W'(I,T)$, respectively, and using the Least-Squared method, we obtained four set of coefficients $[b_{1k}, b_{2k}, \ldots, b_{10k}]$ and $[c_{1k}, c_{2k}, \ldots, c_{10k}]$ for $C_{Mk} = 4$ vol.%, 5 vol.%, 6 vol.%, and 8 vol.% (where $k = 1$, 2, 3, and 4). Using the four set $[b_{1k}, b_{2k}, \ldots, b_{10k}]$ and $[c_{1k}, c_{2k}, \ldots, c_{10k}]$ coefficients, we constructed four fitted *CCSs*(M',I,T) and *CCSs*(W',I,T) as shown in Figs. 9 and 10, respectively. Similar to *CCSs*(I,V,T), before using *ICCS*(M',I,T) and *ICCS*(W',I,T) algorithms to predict M' and W', we need to confirm that no intersection occurs among the four preset *CCSs*(M',I,T) and also among the four preset *CCSs*(W',I,T). Figs. 9 and 10 show no intersection among the four *CCSs*(M',I,T) and also among the four *CCSs*(W',I,T), respectively. Thus the feasible measurement regions for using *CCSs*(M',I,T) and *CCSs*(W',I,T) to predict M' and W' are $T = 30$–$60\,^{\circ}C$, $I = 0.5$–2.5 A, and $C_M = 4.0$–8.0 vol.%.

One thing should be remarked is that the feasible C_M region 4.0–8.0 vol.% of *CCSs*(M',I,T) and *CCSs*(W',I,T) was higher than the feasible C_M region 2.0–6.0 vol.% of *CCSs*(I,V,T) (as shown in Fig. 3). The reasons for the higher C_M regions of *CCSs*(M',I,T) and *CCSs*(W',I,T) than that of *CCSs*(I,V,T) was because that the output voltage was lower than 8.0 V (i.e. the lower bound of feasible voltage region of *CCSs*(I,V,T)) when the DMFC was operated at $I > 2.5$ A and $C_M < 4.0$ vol.%. The low output voltage of the DMFC operated at $I > 2.5$ A was due to the insufficiency of fuel and the high methanol crossover via electro-osmosis when C_M was lower than 4 vol.%. Thus the M' and W' measurements were performed at a region with C_M values higher than 4.0 vol.%. And, the lower and upper bounds of the feasible C_M regions of *CCSs*(M',I,T) and *CCSs*(W',I,T) for predicting M' and W' was higher than those of *CCSs*(I,V,T) for predicting C_M. Combing the feasible C_M region ($C_M = 2.0$–6.0 vol.%) of *ICCS*(I,V,T) and the feasible C_M region ($C_M = 4.0$–8.0 vol.%) of *ICCS*(M',I,T) and *ICCS*(W',I,T), we may conclude the optimum C_M region for using the combined *ICCS*(I,V,T), *ICCS*(M',I,T) and *ICCS*(W',I,T) algorithms for *in situ* fuel control of the present DMFC stack consisting of 32 unit cells is $C_M = 4.0$–6.0 vol.%.

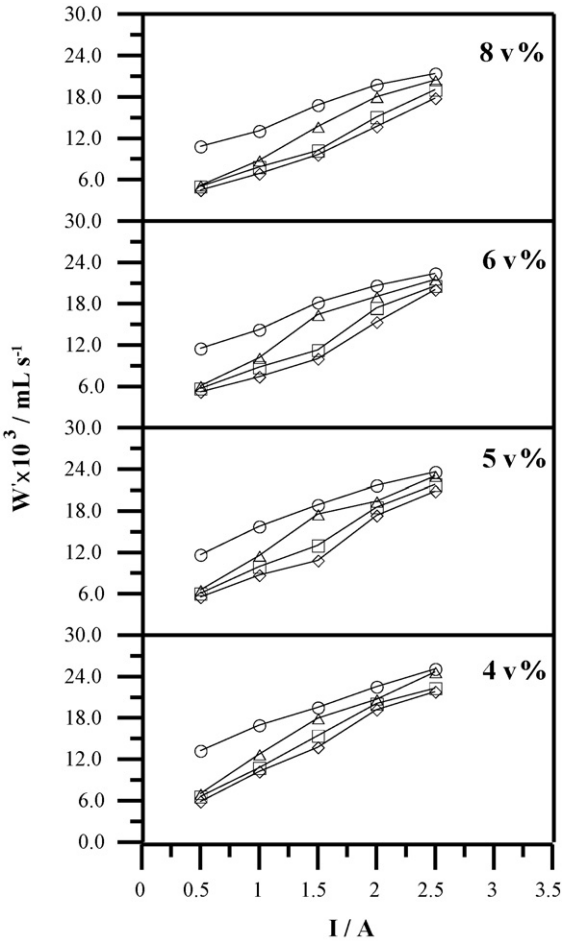

Fig. 8. W' versus I curves obtained at various temperatures with C_M of liquid fuels of 4.0 vol.%, 5.0 vol.%, 6.0 vol.%, and 8.0 vol.% (from bottom to top). Temperature: (◊) 30 °C; (□) 40 °C; (△) 50 °C; (○) 60 °C.

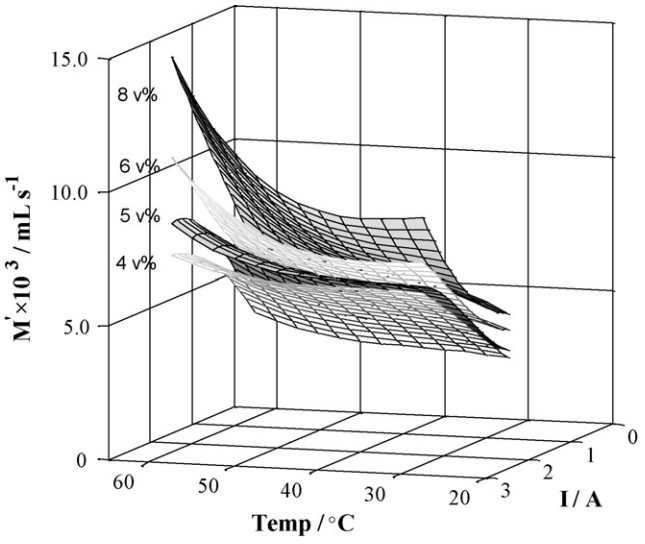

Fig. 9. The fitted $CCS(M',I,T)$ for fuels with C_M = 4.0 vol.%, 5.0 vol.%, 6.0 vol.%, and 8.0 vol.%. The $CCS(M',I,T)$ were constructed using four set $[b_{1k}, b_{2k},\ldots, b_{10k}]$ coefficients (k = 1, 2, 3, and 4) of cubic polynomial of $M'(I,T)$, which were obtained by linear least-square curve fitting of Fig. 7 data.

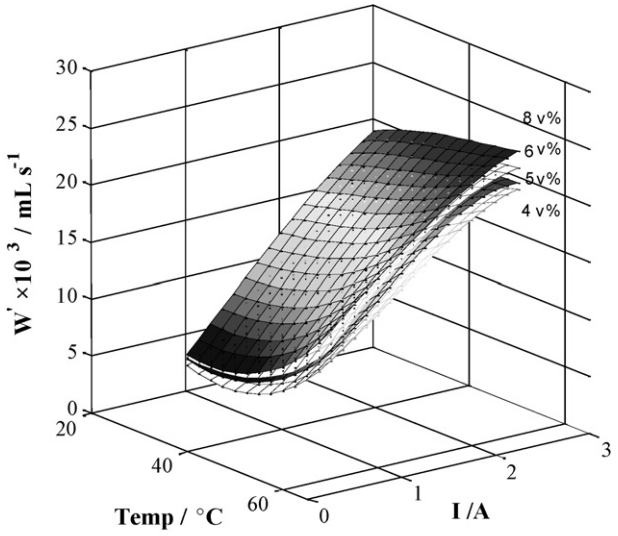

Fig. 10. The fitted $CCS(W',I,T)$ for fuels with C_M = 4.0, 5.0 vol.%, 6.0 vol.%, and 8.0 vol.%. The $CCS(W',I,T)$ were constructed using four set $[c_{1k}, c_{2k},\ldots, c_{10k}]$ coefficients (k = 1, 2, 3, and 4) of cubic polynomial of $W'(I,T)$, which were obtained by linear least-square curve fitting of Fig. 8 data.

7.2.2. Evaluations of ICCS(M′,I,T) and ICCS(W′,I,T) algorithms

To evaluate $ICCS(M',I,T)$ and $ICCS(W',I,T)$ algorithms, three additional methanol concentration levels of liquid fuels (i.e. $C_{M,u}$ = 3.5 vol.%, 4.5 vol.%, and 7.0 vol.%) were introduced to serve as the unknown M_u' and W_u' to be estimated. Each of the three $C_{M,u}$ was assigned 14 testing points distributed in T = 30–60 °C and I = 0.5–2.5 A, and thus 42 sets of measured (M'_u, I_u, T_u) and (W'_u, I_u, T_u) data were obtained. The predicted M_u' and W_u' were calculated using the interpolation Eq. (14) with the pre-established $CCSs(M',I,T)$ (Fig. 9) and the interpolation Eq. (15) with the pre-established $CCSs(W',I,T)$ (Fig. 10), respectively. By comparing the calculated M_u' and W_u' with the measured M_u' and W_u', we estimated the relative errors of calculated M_u' and W_u' data obtained using $ICCS(M',I,T)$ and $ICCS(W',I,T)$ interpolation procedures and show the data of relative errors in Fig. 11. Fig. 11 shows the relative errors of calculated M_u' and W_u' were less than 5.0%, suggesting the accuracy of $ICCS(M',I,T)$ and $ICCS(W',I,T)$ interpolation procedures for predicting M' and W' from I, T, and C_M of the liquid fuel of a DMFC stack consisting of 32 unit cells. For a real-time application of $ICCS(M',I,T)$ and $ICCS(W',I,T)$ interpolation algorithms for *in situ* predicting M' and W', the C_M datum can first be estimated from the *in situ* measured (I,V,T) data using the $ICCS(I,V,T)ICCS(I,V,T)$ algorithm combined with voltage decay correction described in Sections 2 and 3 . The estimated $C_{M,u}$ datum can then be input into $ICCS(M',I,T)$ and $ICCS(W',I,T)$ interpolation algorithms to estimate M' and W', respectively.

7.3. Application of fuel control algorithm to a DMFC stack system

The procedure using $ICCS(I,V,T)$ combined with voltage decay correction, $ICCS(M',I,T)$ and $ICCS(W',I,T)$ algorithms for *in situ* estimation of C_M of the liquid fuel in fuel premixing tank, the cumulated methanol and water consumed quantities of a DMFC system had been described in Section 5. In the present section, a DMFC system consisting of 32 unit cells as shown in Fig. 1 was used to test the stability of the fuel control algorithms. The pre-established voltage decay coefficients are: $e_1 = 5.10 \times 10^{-5}\,\mathrm{V\,s^{-1}}$ and $e_2 = 0.288 \times 10^{-5}\,\mathrm{V\,s^{-1}}$. And, the pre-established coefficients $[a_{1k}, a_{2k},\ldots, a_{10k}]$ of $CCSs(I,V,T)$, the coefficients $[b_{1k}, b_{2k},\ldots, c_{10k}]$ of $CCSs(M',I,T)$, and the coefficients $[c_{1k}, c_{2k},\ldots, c_{10k}]$ of $CCSs(W',I,T)$ were stored in DMFC fuel management system.

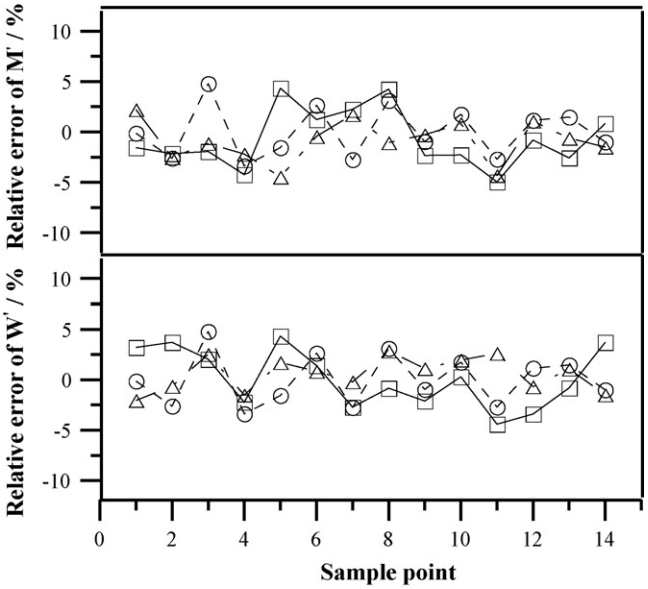

Fig. 11. Relative error of M' (upper graph) and W' (lower graph) estimated using $ICCS(M',I,T)$ (Eq. (14) algorithm with preset$CCS(M',I,T)$ (Fig. 9) and $ICCS(W',I,T)$ (Eq. (15) algorithm with preset $CCS(W',I,T)$ (Fig. 10), respectively. C_M of liquid fuels: (○) 4.5 vol.%; (□) 6.5 vol.%; (△) 7.0 vol.%.

Two power loads were applied on the DMFC testing system. One is a "constant power (16 W) electronic load", the other is a "dynamic power (power varies between 10 W and 15 W) ultra-mobile personal computer with a music player". Fig. 12 shows the 9.5 h testing results of the DMFC stack system under a constant power load of 16 W (Fig. 12 upper graph). The temperature of anode was around 45–48 °C controlled by self-heating from the exothermic heat of the fuel cell (Fig. 12 upper graph). In the fuel premixing tank, the methanol concentration was controlled at $C_M = 5.0 \pm 0.5$ vol.% and the liquid fuel level was controlled at 82 ± 2 vol.% (Fig. 12, lower graph). These results show the C_M and the liquid fuel level in the fuel premixing tank were well controlled and in a stable state when the system was kept at a constant output power.

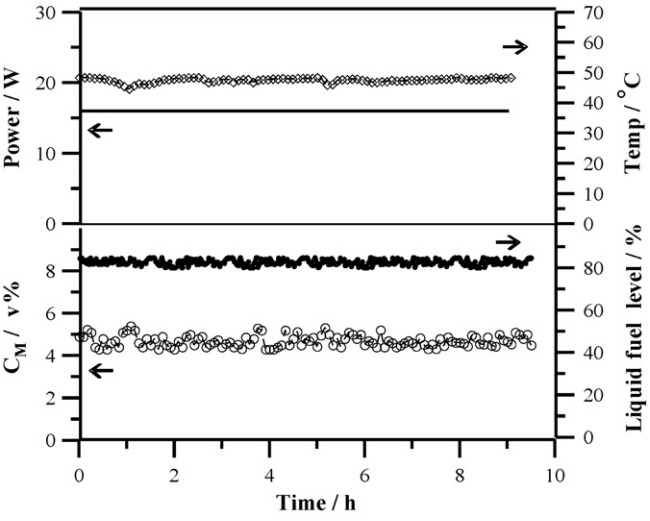

Fig. 12. 9.5 h real-time fuel control test of a DMFC stack using the fuel control algorithms. The applied load was 16 W. (Upper graph) The power load and cell temperature versus fuel cell operating time; (—) loading power; (◊) cell temperature. (Lower graph) C_M and liquid level in the fuel mixing tank versus cell operating time; (○) C_M of liquid fuel in the premixing tank; (●) liquid level in the fuel premixing tank.

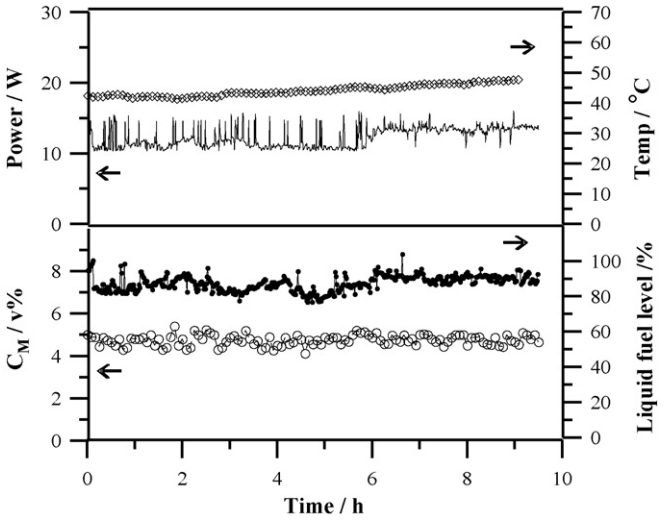

Fig. 13. 9.5 h real-time fuel control test of a DMFC stack using combined $ICCS(I,V,T)ICCS(I,V,T)$ and $ICCS(M',V,T)$ with $ICCS(W',V,T)$ algorithms. The applied load was ultra-mobile personal computer with a dynamic power varied from 10 W to 15 W. (Upper graph) The power load and cell temperature versus fuel cell operating time; (—) loading power; (◊) cell temperature. (Lower graph) Methanol concentration and liquid fuel level in the fuel premixing tank versus cell operating time; (○) C_M of liquid fuel in the premixing tank; (●) liquid fuel level in the fuel premixing tank.

Fig. 13 shows the 9.5 h testing results of the DMFC stack system under a dynamic power load with power varied between 10 W and 15 W. Fig. 13 (upper graph) shows the power was kept at ~11.5 W and fluctuated between 10 W and 15 W in the initial 5.5 h of testing. After 5.5 h, the power increased to 13.5 W with a power fluctuation of 11–16 W. The temperature of the anode was around 42 °C in beginning 2.5 h of testing and then the anode temperature increased slowly from 42 °C to 47 °C when the operating time was from 2.5 h to 9.5 h (Fig. 13, upper graph). In the fuel premixing tank, Fig. 13 (lower graph) shows the C_M was kept at 5.0 ± 0.5 vol.% in the whole period of testing. The liquid fuel level was kept at 87 ± 8% in the initial 5.5 h of testing, then the liquid level increased to 93 ± 5% after 5.5 h of testing. The increment of cell temperature at the latter stage of testing could be due to the increment of power loading. And, the increment of cell temperature might cause an increment of liquid fuel volume and thus an increment of liquid fuel level in the fuel premixing tank after 5.5 h of testing. The increase of input power load also causes more CO_2 gas generation via the anode electrochemical reaction, which also leads to an increment of the liquid fuel level in the fuel premixing tank. The results of a constant $C_M = 5.0 + 0.5$ vol.% and a stable liquid fuel level in the fuel premixing tank during the 9.5 h testing also show the present algorithm is a good fuel control tool of a portable DMFC stack system.

8. Conclusions

In this work, we developed a sensor-less fuel control algorithm for a portable DMFC stack system. The algorithm is a combination of three algorithms, i.e. $ICC(I,V,T)$, $ICCS(M',I,T)$ and $ICCS(W',I,T)$. Instead of the whole experimental data base, only the pre-established coefficients $[e_1, e_2]$ of "*voltage decay*", $[a_{1k}, a_{2k},\ldots, a_{10k}]$ of $ICCS(I,VT)$, $[b_{1k}, b_{2k},\ldots, c_{10k}]$ of $ICCS(M',I,T)$, and $[c_{1k}, c_{2k},\ldots, c_{10k}]$ of $ICCS(W',I,T)$ are needed to be stored for each $C_{M,k}$ ($k = 1, 2,\ldots, n$) in the fuel cell management system. With the pre-established coefficients obtained at available operation regions, $T = 30$–60 °C and $C_M = 4.0$–6.0 vol.%, we showed the "*methanol concentration*" and "*total volume of liquid level*" of the liquid fuel in the fuel premixing tank of a DMFC stack consisting of 32 unit cells were well con-

trolled at $C_M = 5.0 \pm 0.5$ vol.% with the variation of the total liquid volume being less than 8.0 vol.% by the present sensor-less fuel control algorithm when the DMFC system was either loaded with a constant power (16 W) or with a dynamic power (power varies between 10 W and 15 W) for 9.5 h. It is vitally important for a DMFC to monitor the status of the fuel in the system, i.e. the methanol concentration and the remaining amount of liquid fuel solution. The information is the basis of the fuel controlling strategies for a long term self-sustainable DMFC system. A variety of sensing schemes for methanol concentration measurement have been proposed in the literatures. However, less discussion has been referred regarding the remaining amount of the liquid fuel in a DMFC. Most of the electrochemical approaches for detecting methanol concentration had suffered from voltage decay effect, which leads to certain measurement errors and thus confining their feasibility in practical applications. In conclusion, the present paper has achieved the following objectives: (1) Adopting the notion of constant concentration surfaces of Chiu and Lien approach [7]; nevertheless, a compensation scheme to overcome the voltage decay limitation in Chiu and Lien approach is proposed and validated. (2) Providing an approach to evaluate the consumption rate of water and methanol, thereby adequately determining the *in situ* remaining amount of liquid fuel in an operating DMFC system. (3) Validating the proposed approach on a stack of 32-cells for both the steady-state and dynamic operating conditions. Its feasibility from single cell to a practical DMFC system is then further certified. Thus the algorithm is suitable for fuel control management of portable DMFC systems.

Acknowledgement

The authors would like to thank for the financial support of Antig Inc, Taiwan.

References

[1] G. Cacciola, V. Antonucci, S. Freni, J. Power Sources 100 (2001) 67–79.
[2] T. Schultz, S. Zhou, K. Sundmacher, Chem. Eng. Technol. 24 (2001) 1223–1233.
[3] A. Ozeki, U.S. Patent 20060083966 A1 (2006).
[4] C. C. Tung, K. Chien, R.O.C. Patent M313774 (2007).
[5] C.L. Chang, C.Y. Chen, C.C. Sung, D.H. Liou, J. Power Sources 164 (2007) 606–613.
[6] C.Y. Chen, D.H. Liu, C.L. Huang, C.L. Chang, J. Larminie, J. Power Sources 167 (2007) 442–449.
[7] Y.J. Chiu, H.C. Lien, J. Power Sources 159 (2006) 1162–1168.
[8] P. Piela, C. Eickes, E. Brosha, F. Garzon, P. Zelenay, J. Electrochem. Soc. 151 (2004) A2053–A2059.
[9] C. Eickes, P. Piela, J. Davey, P. Zelenay, J. Electrochem. Soc. 153 (2006) A171–A178.
[10] S. Kang, S.J. Lee, H. Chang, J. Electrochem. Soc. 154 (2007) B1179–B1185.
[11] S.C. Thimas, X. Ren, S. Gottesfeld, P. Zelenary, Electrochim. Acta 47 (2002) 3741–3748.
[12] G.Q. Lu, F.Q. Liu, C.Y. Wang, Electrochem. Solid-State Lett. 8 (2005) A1–A4.
[13] W.W. Yang, T.S. Zhao, C. Xu, Electrochim. Acta 53 (2007) 853–862.
[14] J.Y. Park, J.H. Lee, S.K. Kang, J.H. Sauk, I. Song, J. Power Sources 178 (2008) 181–187.